ACS Medicinal Chemistry Letters

Letter

Cite This: ACS Med. Chem. Lett. 2019, 10, 929−935

pubs.acs.org/acsmedchemlett

Synthesis and Optimization of K_v7 (KCNQ) Potassium Channel Agonists: The Role of Fluorines in Potency and Selectivity

Ruiting Liu,[†] Thanos Tzounopoulos,[‡] and Peter Wipf*[,†]

[†]Department of Chemistry, University of Pittsburgh, Pittsburgh, Pennsylvania 15260, United States

[‡]Department of Otolaryngology, School of Medicine, University of Pittsburgh, Pittsburgh, Pennsylvania 15260, United States

Supporting Information

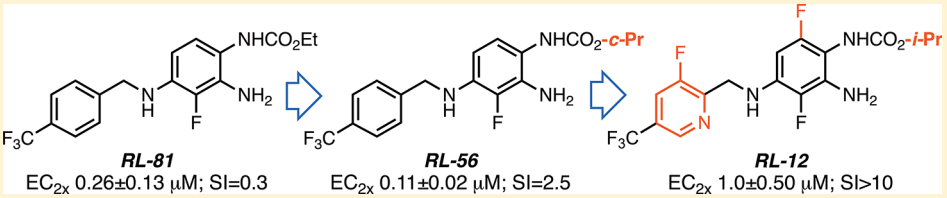

ABSTRACT: Based on the potent K_v7 agonist **RL-81**, we prepared new lead structures with greatly improved selectivity for $K_v7.2/K_v7.3$ over related potassium channels, i.e., $K_v7.3/K_v7.5$, $K_v7.4$, and $K_v7.4/7.5$. **RL-36** and **RL-12** maintain an agonist EC_{2x} of ca. 1 μM on $K_v7.2/K_v7.3$ in a high-throughput assay on an automated electrophysiology platform in HEK293 cells but lack activity on $K_v7.3/K_v7.5$, $K_v7.4$, and $K_v7.4/7.5$, resulting in a selectivity index SI > 10. **RL-56** is remarkably potent, EC_{2x} 0.11 ± 0.02 μM, and still shows an SI = 2.5. We also identified analogues with significant selectivity for $K_v7.4/K_v7.5$ over $K_v7.2/K_v7.3$. The extensive use of fluorine in iterative core structure modifications highlights the versatility of these substituents, including F, CF_3, and SF_5, to span orders of magnitude of potency and selectivity in medicinal chemistry lead optimizations.

KEYWORDS: *K_v7, KCNQ, potassium channel agonist, retigabine, RL-81*

Potassium channels represent the most numerous group among the ca. 150 cation channels expressed in the human genome. They trigger a multitude of physiological responses, such as the frequency and duration of action potentials in the brain and heart, muscle contraction, transmitter release, and hormonal secretion. In this realm, the five distinct voltage-dependent K_v7 channel subunits, encoded by the *KCNQ* genes in humans, are of considerable interest to medicinal chemists. To a significant extent, this is due to their close association with various diseases as well as the tractability of their pharmacological response to small-molecule modifiers.[1] Epilepsy, neuropathic pain, tinnitus, migraine, and cardiovascular, metabolic, and psychiatric diseases are frequently associated with defective K_v7 channels.[2] The $K_v7.1$ subtype is primarily located in the cell membranes of cardiac tissue and is critical for the repolarization of the cardiac action potential; aberrations can lead to a prolongation of the QT interval. $K_v7.2-K_v7.5$ are active in neuronal tissue, and $K_v7.4$ and $K_v7.5$ are also expressed in skeletal and smooth muscle cells. The neuronal channels are assembled as homo- or heterotetramers; i.e., they form $K_v7.2/K_v7.3$, $K_v7.3/K_v7.4$, $K_v7.4/K_v7.5$, etc., channel complexes.[1,3]

$K_v7.2/K_v7.3$ heterotetramers are slow-activating, voltage-dependent, non-inactivating potassium channels that are open at hyperpolarizing (subthreshold) potentials. Accordingly, they control the subthreshold membrane potential and serve as powerful brakes on neuronal firing activity. Genetic or acquired reductions in the activity of $K_v7.2/K_v7.3$ heterodimers, underlying native K_v7 currents in neurons,[4] are linked with brain disorders that are characterized by neuronal hyperexcitability, including anxiety, mania, tinnitus, and ADHD.[5] Consequently, $K_v7.2-K_v7.5$ channel activators are capable of compensating for a constitutive decline in K_v7 channel activity and thus decrease neuronal excitability and block neurotransmitter release.[3] Flupirtine, retigabine, P-retigabine, SF-0034, acrylamide (*S*)-1, SMB-1, γ-aminobutyric acid (GABA), gabapentine, ICA-27243, diclofenac, BMS-204352, celecoxib, ML-213, NS-1643, and compound 14 are representative structures for the chemical space covered by small-molecule K_v7 activators (Figure 1).[3,6−8]

Pharmacological activation of K_v7 channels by retigabine, an FDA-approved antiepileptic drug that serves as a pan-agonist at $K_v7.2-K_v7.5$ channels, prevents seizures, neuropathic pain, and the development of tinnitus.[9,10] In the CNS of vertebrates, $K_v7.2/K_v7.3$ (KCNQ2/3) propagate the M-current, a muscarinic-inhibited trigger of neuronal excitability. Moreover, natural, nonpharmacologically driven recovery in $K_v7.2/K_v7.3$ channel activity is linked to resilience to noise-induced tinnitus.[11] However, the possibility for severe side effects with retigabine, including urinary retention, blue skin, and retinal discoloration, resulted in a "black box" warning by the FDA for this drug, at first limiting its use to patients who had not responded to alternative treatments, until the drug was discontinued in 2017.[12] We hypothesized that these undesir-

Received: March 8, 2019
Accepted: May 8, 2019
Published: May 8, 2019

DOI: 10.1021/acsmedchemlett.9b00097
ACS Med. Chem. Lett. 2019, 10, 929−935

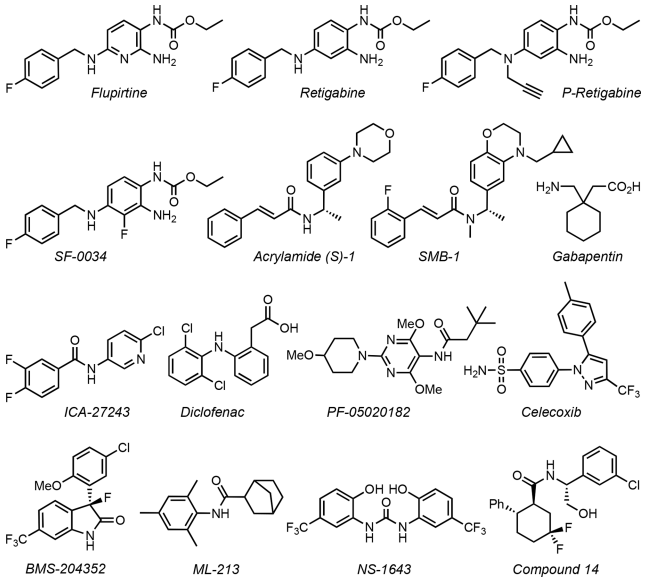

Figure 1. Structures of K_v7 channel activators.

able side effects were due in part to the poor selectivity of retigabine among $K_v7.2-K_v7.5$ channels as well as the low solubility of its metabolic degradation products. Interestingly, exposure of retigabine to a hypervalent iodine reagent as a model for the oxidative metabolism of xenobiotic substances[13] generated the colored, poorly soluble dimer **2**, whose structure was confirmed by X-ray analysis (Scheme 1). Dimer **2** has also been identified as an impurity in the retigabine API.[14]

Scheme 1. Oxidation of Retigabine and X-ray Structure of Symmetrical Dimer 2

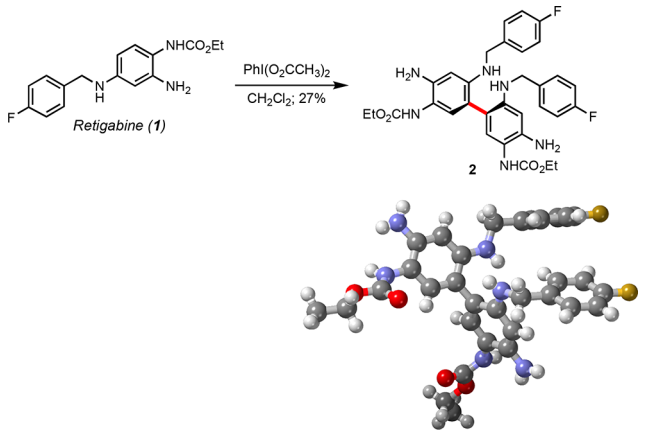

To generate potent $K_v7.2/K_v7.3$-selective channel activators, we previously partitioned retigabine's chemical structure into three distinct zones (Figure 2).[15] In these preliminary structure–activity relationship (SAR) studies, we mainly modified zones 1 and 3 and subsequently combined the beneficial modifications found for zones 1 and 3 with a previously known beneficial modification on zone 2, which had also been used in the development of the retigabine analogue SF-0034.[10] Our guiding principle for these preliminary SAR studies was to modulate both steric and, in particular, electronic features in zone 1 by introducing fluoride (F), trifluoromethyl (CF_3), and pentafluorosulfanyl (SF_5), which is considered a "super-trifluoromethyl" substituent.[16,17] This

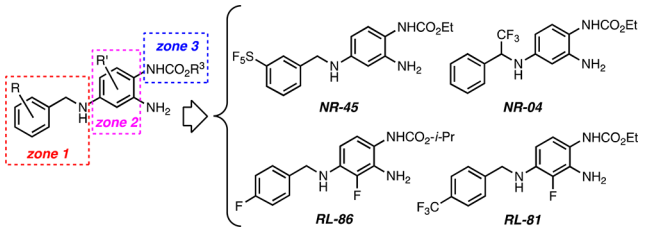

Figure 2. Structures of K_v7 channel activating retigabine analogs.

strategy led us to the potent and selective benzylamines **NR-45**, **NR-04**, and **RL-86** (Figure 2).[15] Furthermore, by introducing a CF_3 group at the 4-position of the benzylamine moiety, combined with a fluorine atom at the 3-position of the aniline ring, we generated **RL-81**, a new $K_v7.2/K_v7.3$-specific activator (EC_{50} = 190 nM) that was ca. 3 times more potent than the most active retigabine analogue, SF-0034 (EC_{50} = 0.60 μM), at shifting the voltage dependence of $K_v7.2/K_v7.3$ channels to more hyperpolarized potentials.[15] Hence, **RL-81** became a promising lead structure for the development of clinical candidates for treating or preventing neurological disorders associated with neuronal hyperexcitability, including tinnitus and epilepsy.

With **RL-81** as a new lead, we focused our attention on zone 2 modifications, in particular the position and the number of fluorine groups on the three unsubstituted carbons of the triaminobenzene moiety, in part motivated by the goal to find potent analogues where the dimerization site in **2** was blocked. We also reoptimized structural features of zone 1 and zone 3 and developed a computational SAR model.

The syntheses of **RL-81** and 19 new analogues are summarized in Schemes 2–5. S_NAr of benzylamines **3a–3c**

Scheme 2. Preparation of RL-81 and 6 Structurally Closely Related Analogues from Monosubstituted Benzylamines 3a–3c

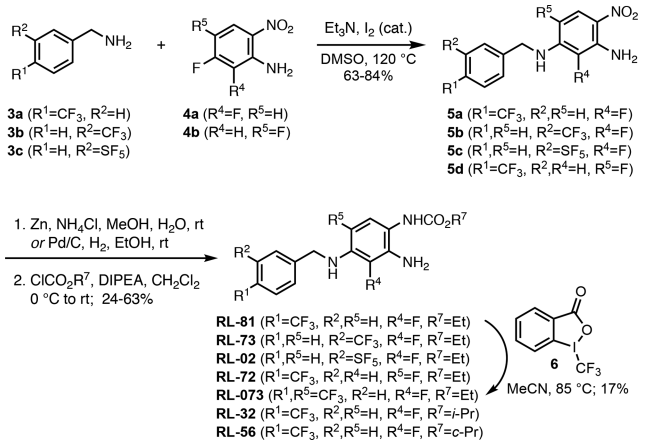

with fluoroarenes **4a** and **4b** in the presence of catalytic iodine generated anilines **5a–5d** in 63–84% yield (Scheme 2). Reduction of the nitro group and treatment with ethyl chloroformate led to **RL-81**, **RL-73**, **RL-02**, and **RL-72** in 47%, 45%, 37%, and 24% yield, respectively. **RL-81** was treated with Togni's trifluoromethylating reagent **6**[18] in acetonitrile to obtain the R^5 trifluoromethyl derivative **RL-073**, albeit in a low yield of 17%. For the preparation of the zone 3 modified *iso*-propyl and *cyclo*-propyl carbamates **RL-32** and **RL-56**, nitroaniline **5a** was reduced with Pd/C under an atmosphere

DOI: 10.1021/acsmedchemlett.9b00097
ACS Med. Chem. Lett. 2019, 10, 929–935

of hydrogen gas in ethanol, and the resulting diamine was selectively acylated with *iso*-propyl chloroformate and *cyclo*-propyl chloroformate in 63% and 40% yield, respectively.

The use of 2-fluoro-4-trifluoromethylbenzylamine **3d** introduced an additional fluorine group into the zone 1 moiety, and in an analogous series of S_NAr, zinc reduction, and carbamoylation transformations, ethyl carbamate **RL-18** and *cyclo*-propyl carbamates **RL-35**, **RL-36**, **RL-46**, and **RL-50** were obtained in moderate to good yields (Scheme 3). In this series of analogues, we also introduced up to two additional fluorine substituents at zone 2 R^5 and R^6 positions.

Scheme 3. Preparation of 5 Analogues Containing the 2-Fluoro-4-trifluoromethylbenzylamine Moiety in Zone 1

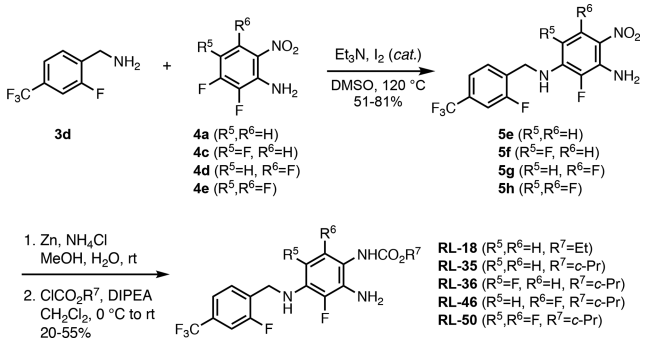

3d

4a (R^5,R^6=H)
4c (R^5=F, R^6=H)
4d (R^5=H, R^6=F)
4e (R^5,R^6=F)

5e (R^5,R^6=H)
5f (R^5=F, R^6=H)
5g (R^5=H, R^6=F)
5h (R^5,R^6=F)

RL-18 (R^5,R^6=H, R^7=Et)
RL-35 (R^5,R^6=H, R^7=*c*-Pr)
RL-36 (R^5=F, R^6=H, R^7=*c*-Pr)
RL-46 (R^5=H, R^6=F, R^7=*c*-Pr)
RL-50 (R^5,R^6=F, R^7=*c*-Pr)

A further diversification of the **RL-81** lead structure was accomplished by the use of (5-(trifluoromethyl)pyridin-2-yl)methanamine **3e** and (3-fluoro-5-(trifluoromethyl)pyridin-2-yl)methanamine **3f** (Scheme 4). Reduction of the nitro

Scheme 4. Preparation of 5 Analogues Containing the 2-Pyridylmethylamine Moiety in Zone 1

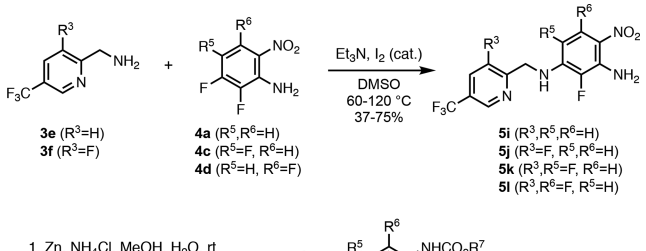

3e (R^3=H)
3f (R^3=F)

4a (R^5,R^6=H)
4c (R^5=F, R^6=H)
4d (R^5=H, R^6=F)

5i (R^3,R^5,R^6=H)
5j (R^3=F, R^5,R^6=H)
5k (R^3,R^5=F, R^6=H)
5l (R^3,R^6=F, R^5=H)

RL-31 (R^3,R^5,R^6=H, R^7=Et)
RL-68 (R^3,R^5,R^6=H, R^7=*c*-Pr)
RL-96 (R^3=F, R^5,R^6=H, R^7=*c*-Pr)
RL-01 (R^3,R^5=F, R^6=H, R^7=*c*-Pr)
RL-12 (R^3,R^6=F, R^5=H, R^7=*c*-Pr)

group in **5i**, isolated in 75% yield from the coupling of **3e** with **4a**, with Pd/C and acylation with ethyl chloroformate provided **RL-31** in 43% yield. A zinc reduction and *cyclo*-propyl chloroformate were used for the preparation of **RL-68** in 23% yield from **5i**. The *penta*- and *hexa*-fluorinated intermediates **5j**, **5k**, and **5l** were obtained from the coupling of **3f** with **4a**, **4c**, and **4d** in 45%, 58%, and 37% yield, respectively. Zinc reduction and treatment with *cyclo*-propyl chloroformate then yielded the corresponding carbamates **RL-96**, **RL-01**, and **RL-12** in 33%, 37%, and 41%, respectively.

Finally, we also synthesized analogues with a pyridine in zone 1 by coupling of amine **3g** with nitrobenzene **4a**, which gave S_NAr product **5m** in 85% yield (Scheme 5). Reduction and acylation of **5m** provided the carbamates **RL-24** and **RL-67** in 60% and 28% yield, respectively. The 2-pyridyl analogue **RL-23**, which also contained a cyano group next to the nitrogen of the heterocycle as a chemical replacement mimicking a pyridazine ring,[19] was generated in an overall yield of 13% by a reductive amination of pyridine **3h** with aniline **4f**, followed by zinc reduction and acylation.

Scheme 5. Preparation of 3 Analogues Containing the 3-Pyridylmethylamine and the 3-Cyano-2-pyridylmethylamine Moieties in Zone 1

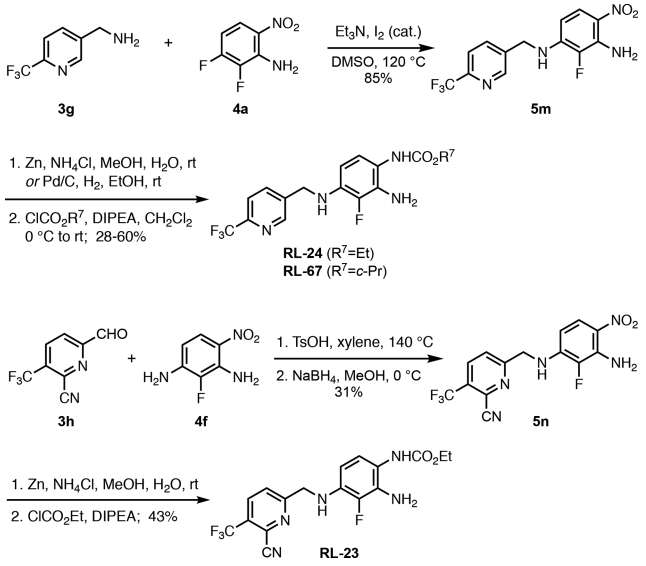

3g
4a
5m
RL-24 (R^7=Et)
RL-67 (R^7=*c*-Pr)
3h
4f
5n
RL-23

The biological evaluation of the new analogues, including **RL-81** as a positive standard, was performed in the Lilly OIDD program.[20,21] Ion channel agonistic potency was determined in a high-throughput assay using the automated electrophysiology IonWorks Barracuda (IWB) platform in HEK293 cells (Table 1). The resulting 10-point concentration−response curves provide a measure of compound efficacy by determining the agonist concentration that doubles the conductance at the voltage leading to 15% channel activation (EC_{2x}).[22] When the EC_{2x} value is lower, the agonist is more potent.

Compared to the literature standards, flupirtine (FP) and retigabine (RG), our previous lead structure **RL-81** demonstrated ca. 8−50 times higher (vs FP) or slightly higher (vs RG) efficacy at all tested K_v7 channels (Table 1) in this assay. Since we were mainly interested in optimizing central ($K_v7.2$/$K_v7.3$) over peripheral ($K_v7.4$/$K_v7.5$) tissue activities, we also calculated a selectivity index (SI), defined as the inverse ratio of the EC_{2x} values for these two channel types (i.e., SI = $EC_{2x}(K_v7.4/K_v7.5)/EC_{2x}(K_v7.2/K_v7.3)$; when this ratio is higher, the selectivity of the agent for the $K_v7.2/K_v7.3$ channels is better). Interestingly, **RL-81** (SI = 0.3) proved to be considerably more potent at $K_v7.4/K_v7.5$ than FP (SI = 1.8), suggesting a potentially adverse property profile and setting the stage for further medicinal chemistry optimizations. One of our first modifications was to move the CF_3 group in zone 1 in **RL-81** from the *para*- to the *meta*-position. To our delight, the resulting analogue, **RL-73**, was twice as potent at $K_v7.2/K_v7.3$ than **RL-81**, while substantially decreasing activity at $K_v7.4/K_v7.5$, resulting in a superior SI = 4.7. These findings were further substantiated by the SF_5-containing analogue **RL-02**,

DOI: 10.1021/acsmedchemlett.9b00097
ACS Med. Chem. Lett. 2019, 10, 929−935

Table 1. Efficacy of RL-81 Analogues in Human K_v7 Channel Conductance Studies[a]

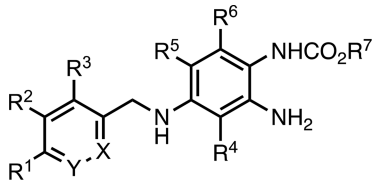

compd	X	Y	R^1	R^2	R^3	R^4	R^5	R^6	R^7	$K_v7.2/3$ EC_{2x} ± SD [μM]	$K_v7.3/5$ EC_{2x} ± SD [μM]	$K_v7.4$ EC_{2x} ± SD [μM]	$K_v7.4/5$ EC_{2x} ± SD [μM]	SI
FP	CH	CH	F	H	H	N[b]	H	H	Et	2.00 ± 0.69	1.58 ± 0.69	5.62 ± 1.86	3.50 ± 2.68	1.8
RG	CH	CH	F	H	H	H	H	H	Et	0.33 ± 0.08	0.34 ± 0.04	ND	ND	ND
RL-81	CH	CH	CF_3	H	H	F	H	H	Et	0.26 ± 0.13	0.29 ± 0.06	0.10 ± 0.04	0.09 ± 0.04	0.3
RL-73	CH	CH	H	CF_3	H	F	H	H	Et	0.14 ± 0.05	0.20 ± 0.08	0.40 ± 0.13	0.66 ± 0.01	4.7
RL-02	CH	CH	H	SF_5	H	F	H	H	Et	0.36 ± 0.25	0.21 ± 0.11	0.65 ± 0.39	0.65 ± 0.28	1.8
RL-72	CH	CH	CF_3	H	H	H	F	H	Et	1.26 ± 0.31	>10	4.65 ± 0.95	>10	>7
RL-073	CH	CH	CF_3	H	H	F	CF_3	H	Et	>10	>10	>10	>10	ND
RL-32	CH	CH	CF_3	H	H	F	H	H	*i*-Pr	0.16 ± 0.11	0.16 ± 0.10	0.19 ± 0.10	4.98 ± 1.12	31
RL-56	CH	CH	CF_3	H	H	F	H	H	*c*-Pr	0.11 ± 0.02	0.23 ± 0.10	0.38 ± 0.30	0.28 ± 0.03	2.5
RL-18	CF	CH	CF_3	H	H	F	H	H	Et	0.18 ± 0.11	0.34 ± 0.01	0.11 ± 0.04	0.30 ± 0.26	1.7
RL-35	CF	CH	CF_3	H	H	F	H	H	*c*-Pr	0.59 ± 0.08	0.47 ± 0.01	0.21 ± 0.19	0.35 ± 0.17	0.6
RL-36	CF	CH	CF_3	H	H	F	F	H	*c*-Pr	0.93 ± 0.21	>10	>10	>10	>10
RL-46	CF	CH	CF_3	H	H	F	H	F	*c*-Pr	1.47 ± 0.22	>10	0.55 ± 0.14	>10	>7
RL-50	CF	CH	CF_3	H	H	F	F	F	*c*-Pr	>10	>10	>10	>10	ND
RL-31	N	CH	CF_3	H	H	F	H	H	Et	0.66 ± 0.25	0.79 ± 0.26	0.85 ± 0.14	0.59 ± 0.34	0.9
RL-68	N	CH	CF_3	H	H	F	H	H	*c*-Pr	0.79 ± 0.03	0.72 ± 0.05	0.90 ± 0.02	0.96 ± 0.05	1.2
RL-96	N	CH	CF_3	H	F	F	H	H	*c*-Pr	1.39 ± 0.20	>10	>10	>10	>7
RL-01	N	CH	CF_3	H	F	F	F	H	*c*-Pr	>10	>10	>10	>10	ND
RL-12	N	CH	CF_3	H	F	F	H	F	*c*-Pr	1.00 ± 0.50	>10	>10	>10	>10
RL-23	N	CCN	CF_3	H	H	F	H	H	Et	1.60 ± 0.19	1.30 ± 0.16	2.17 ± 0.37	2.33 ± 0.89	1.5
RL-24	CH	N	CF_3	H	H	F	H	H	Et	0.61 ± 0.34	0.69 ± 0.35	0.95 ± 0.13	1.27 ± 0.05	2.1
RL-67	CH	N	CF_3	H	H	F	H	H	*c*-Pr	0.71 ± 0.23	0.69 ± 0.19	1.13 ± 0.72	1.36 ± 0.70	1.9

[a] EC_{2x} data were obtained from 10-point concentration curves and 2−5 individual assay determinations, with the exception of FP, for which 6−431 repeats were determined; SD = standard deviation; SI = selectivity index = $EC_{2x}(K_v7.4/5)/EC_{2x}(K_v7.2/3)$; ND = not determined. [b] FP has a pyridine ring nitrogen at the R^4-substituted carbon position.

which showed an equivalent channel activity profile to **RL-73** and also had a more favorable SI = 1.8. Since structurally the only difference between **RL-73** and **RL-02** is the switch from a *meta*-CF_3- to a *meta*-SF_5-substituent in zone 1, these assay data further validate the potential for biological mimicry between the trifluoromethyl and the pentafluorosulfanyl groups.[16,17] Interestingly, while their $K_v7.2/K_v7.3$ vs $K_v7.4/K_v7.5$ selectivity is high, both **RL-73** and **RL-02** have low EC_{2x} values for $K_v7.3/K_v7.5$ and $K_v7.4$ in the 0.2−0.6 μM range, comparable to **RL-81**'s EC_{2x} of 0.29 and 0.10 μM. Therefore, we continued our structure−activity studies and prepared several zone 2 and zone 3 modifications of **RL-81**.

Moving the fluorine atom from R^4 to R^5 in **RL-72** had a detrimental effect on the EC_{2x} for $K_v7.2/K_v7.3$, reducing it 5-fold vs **RL-81** to 1.26 μM. However, the selectivity was now superb, with EC_{2x}'s of >10, 4.65, and >10 μM for $K_v7.3/K_v7.5$, $K_v7.4$, and $K_v7.4/7.5$, respectively, accounting for an SI > 7. In contrast, installing a CF_3 group at the R^5 position in **RL-073** completely abrogated activity at all channel types. This position appears to be very sensitive to steric bulk.

Surprisingly, changing the ethyl carbamate in zone 3 to an *iso*-propyl carbamate slightly increased the potency of the resulting **RL-32** at $K_v7.2/K_v7.3$ but vastly decreased the $K_v7.4/7.5$ EC_{2x} to 4.98 μM, leading to an SI = 31−two orders of magnitude better than the SI = 0.3 of **RL-81**. The SI = 2.5 of the corresponding *cyclo*-propyl carbamate analogue, **RL-56**, fits this trend, since the steric dimensions of a *cyclo*-propane are roughly in between those of the *iso*-propane and the ethane groups. **RL-56** proved to be the most active analogue on $K_v7.2/K_v7.3$ prepared to date, with an EC_{2x} of 0.11 ± 0.02 μM. However, both **RL-32** and **RL-56** also still showed <0.4 μM EC_{2x} potencies at $K_v7.3/K_v7.5$ and $K_v7.4$ channels.

For the next SAR iteration, we introduced a 2-fluoro-4-trifluoromethylbenzylamine moiety in zone 1 and systematically varied fluorinations in zone 2. The parent compound in this series, **RL-18**, was both potent, EC_{2x} = 0.18 ± 0.11 μM, and moderately selective, SI = 1.7 (Table 1). Changing the ethyl to the *cyclo*-propyl carbamate decreased potency and SI (i.e., **RL-35**), but as previously found, adding fluorine at R^5 or R^6 recovered a high selectivity, generating an SI > 10 and SI > 7, respectively, for **RL-36** and **RL-46**. In agreement with the data found for **RL-72**, the R^5-fluorinated **RL-36** also lacked agonist activity at $K_v7.3/K_v7.5$, $K_v7.4$, and $K_v7.4/7.5$, and due to its remaining sub-micromolar EC_{2x} = 0.93 at $K_v7.2/K_v7.3$, **RL-36** therefore represents an overall significant improvement over **RL-81**. In contrast, the *hepta*-fluorinated **RL-50** lost all activity at these channels.

In a final round of SAR investigations, we replaced the trifluorobenzene in zone 1 with trifluoromethylated pyridines. Initially, we focused on the 2-pyridyl analogues **RL-31**, **RL-68**, **RL-96**, **RL-01**, **RL-12**, and **RL-23**. With the exception of the R^3-fluorinated **RL-96** and **RL-12**, these analogues demon-

DOI: 10.1021/acsmedchemlett.9b00097
ACS Med. Chem. Lett. 2019, 10, 929−935

strated either low selectivity or low potency. The R^3,R^4,R^6-trifluorinated **RL-12**, in particular, maintained a respectable 1.00 μM EC_{2x} at $K_v7.2/K_v7.3$, with an SI > 10 and no detectable agonist activity at other channels. Compared to their 2-pyridyl isomers **RL-31** and **RL-68**, the 3-pyridyl analogues **RL-24** and **RL-67** showed slightly increased selectivity but essentially equivalent potency, demonstrating that, among the studied chemotypes, the fluorination pattern was the most significant determinant of selectivity and activity.

Since substitution with fluorine has profound effects on the electron distribution in conjugated π-systems, we examined the electrostatically encoded electron-density surfaces of **RL-81** vs **RL-50**, which has additional fluorinations at the benzylamine moiety and, especially, at R^5 and R^6 of the triaminobenzene, rendering it inactive at all K_v7 channel types (Figure 3). Most

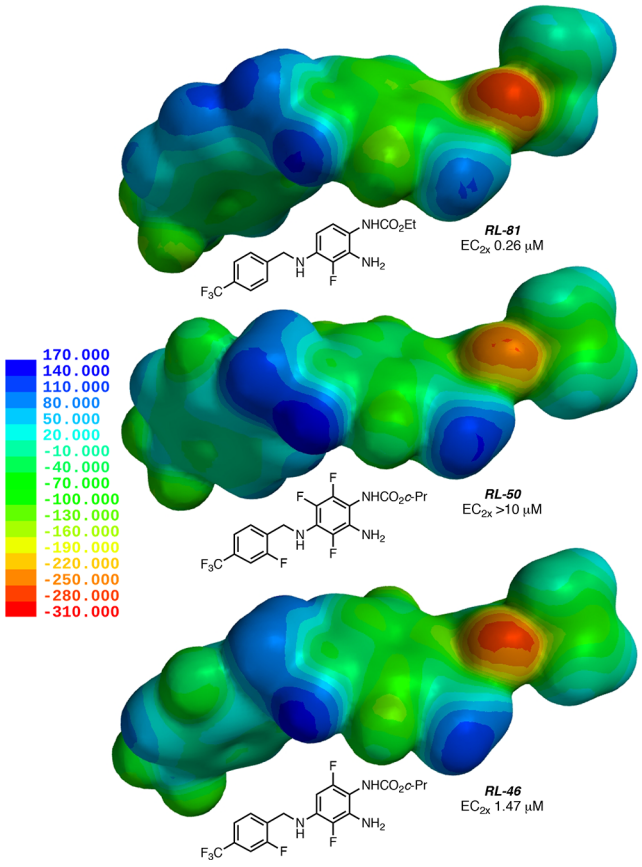

Figure 3. Maps of the electron-density surface encoded with electrostatic potential for **RL-81** (top), **RL-50** (middle), and **RL-46** (bottom). Colors reflect a property range from +170 kJ/mol (blue) to −310 kJ/mol (red).[25]

significantly, the electron density at the carbamate oxygen and the *ortho*-aniline nitrogen is significantly decreased as a result of the two additional fluorinations at the triaminobenzene moiety in **RL-50**. In comparison, **RL-46**, which only has one additional fluorine atom at R^6 vs **RL-81** and is still quite active, shows an intermediate electron density at the carbamate oxygen and the *ortho*-aniline nitrogen. We briefly also explored the possibility that a hindered rotation at the zone 1 benzylamine moiety could be responsible for the lack of activity of the *o*,*o*′-disubstituted aniline **RL-50**. However, a potential energy analysis (HF-6-31G*) suggested a barrier of only 1.5−2.5 kcal/mol for the C−NH−CH_2−C dihedral angle for both **RL-50** and the *o*-monosubstituted reference compound **RL-46** and geometrically similar energy minima.[21] Accordingly, we hypothesize that $K_v7.2$−5 channel potency is largely due to the electrostatic/H-bonding interactions at the carbamate oxygen and the *ortho*-aniline, with decreased electron density being detrimental. In contrast, steric and conformational effects at the carbamate and the benzylamine moieties appear to influence channel selectivity. This rationalization is also supported by literature evidence. On the basis of mutation and modeling studies, the tryptophan residue W236 in $K_v7.2$ (or, analogously and respectively, W265, W242, and W235 in $K_v7.3$, $K_v7.4$, and $K_v7.5$) is thought to be critical for binding and participates in hydrogen bonding interactions with carbamate or amide groups of small-molecule agonists.[23,24] In contrast, $K_v7.1$, which lacks a corresponding W residue, is not activated by retigabine-type molecules.

An alternative, but possibly complementary, interpretation of the differential selectivities observed for fluorinated and heterocyclic analogues of retigabine and **RL-81** could be their preference for different binding sites on the channels and hence different mechanisms of action. While retigabine binds to the pore domain on $K_v7.2$−$K_v7.5$, other compounds have been suggested to target the voltage-sensing domain.[26] In the future, we plan to perform experimental and computational studies to further investigate this hypothesis on our lead compounds.

In conclusion, we have prepared and characterized analogues of the potent K_v7 agonist **RL-81** and obtained several new lead structures with greatly improved selectivity for $K_v7.2/K_v7.3$ over the other tested potassium channels, i.e., $K_v7.3/K_v7.5$, $K_v7.4$, and $K_v7.4/7.5$. Specifically, **RL-36** and **RL-12** maintain an agonist EC_{2x} of ca. 1 μM on $K_v7.2/K_v7.3$ in a high-throughput assay on the automated IWB platform in HEK293 cells but lack activity on $K_v7.3/K_v7.5$, $K_v7.4$, and $K_v7.4/7.5$, resulting in a selectivity index SI > 10. We have also identified an analogue of **RL-81**, i.e., **RL-56**, with a ca. 3 times more potent EC_{2x} of 0.11 ± 0.02 μM. Furthermore, **RL-56** also shows an SI = 2.5 for $K_v7.2/K_v7.3$ over $K_v7.4/K_v7.5$; i.e., it is almost an order of magnitude more selective than **RL-81** (SI = 0.3). Accordingly, **RL-56**, **RL-36**, and **RL-12** represent promising new lead structures for the therapeutic use of selective potassium channel agonists in epilepsy, neuropathic pain, anxiety, mania, ADHD, depression, migraines, and tinnitus. It is also worth mentioning that the R^5 substitution on **RL-36** should prevent the oxidative dimerization observed for RG; further studies to test this hypothesis, including *in vivo* metabolite identification, are planned. In a preliminary experiment, subjecting **RL-36** and the R^5,R^6-difluorinated **RL-50** to the oxidative conditions from Scheme 1 did not produce a corresponding dimer product by LCMS analysis, and starting materials were recovered in 43% and 51% yield, respectively, based on NMR integration of the crude reaction mixture in the presence of an internal standard. A metabolic stability analysis of RG, **RL-81**, and eight analogues in pooled human (HLM) and male mouse (MLM) liver microsomes suggested that the pyridine-containing **RL-24** (HLM $t_{1/2}$ = 406 min) and the *iso*-propyl carbamate **RL-32** (HLM $t_{1/2}$ = 451 min) have longer half-lives than **RL-81** (HLM $t_{1/2}$ = 344 min). Only the *cyclo*-propyl carbamate **RL-36** (HLM $t_{1/2}$ = 76 min) has a substantially shorter half-live than **RL-81**, but the microsomal degradation of all tested analogues is significantly faster than RG (HLM $t_{1/2}$ = 970 min), which we hypothesize will prove advantageous in overcoming RG's undesired

DOI: 10.1021/acsmedchemlett.9b00097
ACS Med. Chem. Lett. 2019, 10, 929−935

toxicities (see Tables S1 and S2 in the Supporting Information for comprehensive HLM and MLM data).

Our SAR analysis demonstrates the ability of fluorine substituents to substantially alter the potency and selectivity of pharmaceutical candidates. While the utility of fluorinated drug candidates has been highlighted in particular for their increases in metabolic stability, conformational effects, and pK_a modulation and for applications as bioisosteric replacements, fewer studies have focused on their effects on specific target affinity.[27] The extensive use of fluorine as the guiding principle in iterative core structure modifications in this work further supports the versatility of fluorine-containing substituents, including F, CF_3, and SF_5, to span orders of magnitude of potency and selectivity in lead optimization.

While our primary goal was the preparation of a K_v7 agonist with a high selectivity for $K_v7.2/K_v7.3$ over $K_v7.4/K_v7.5$, we note that this work also identified several analogues with significant selectivity for $K_v7.4/K_v7.5$ over $K_v7.2/K_v7.3$, i.e., compounds with an SI < 1, such as **RL-81** and **RL-35**. $K_v7.4$ is the primary potassium channel in the smooth muscle of the bladder, where it serves to regulate contractility.[28] Activation of $K_v7.4$ leads to membrane hyperpolarization and a resultant loss of contractile function, a possible etiology for the urinary retention side effect of RG. While currently there is no clinical precedence for selective agonists of $K_v7.4$ and $K_v7.5$, other medicinal chemistry efforts toward this goal have been reported.[29] Therefore, **RL-81** and **RL-35** could form a foundation for the development of much more selective $K_v7.4/K_v7.5$ activators, with potential applications for the treatment of visceral smooth-muscle-related diseases.

■ ASSOCIATED CONTENT

Supporting Information

The Supporting Information is available free of charge on the ACS Publications website at DOI: 10.1021/acsmedchemlett.9b00097.

Experimental details and ^1H and ^{13}C NMR spectra for new synthetic intermediates and products, assay information from the Eli Lilly OIDD program, and details of dihedral angle conformational analysis (PDF)

■ AUTHOR INFORMATION

Corresponding Author

*E-mail: pwipf@pitt.edu.

ORCID

Peter Wipf: 0000-0001-7693-5863

Author Contributions

The manuscript was written through contributions of all authors. All authors have given approval to the final version of the manuscript.

Funding

This work was supported in part by DOD Award W81XWH-18-1-0623 (to T.T. and P.W.).

Notes

The authors declare no competing financial interest.

CCDC 1899172 contains the supplementary crystallographic data for this paper. These data can be obtained free of charge via www.ccdc.cam.ac.uk/data_request/cif, or by emailing data_request@ccdc.cam.ac.uk, or by contacting The Cambridge Crystallographic Data Centre, 12 Union Road, Cambridge CB2 1EZ, U.K.; fax: + 44 1223 336033.

■ ACKNOWLEDGMENTS

OIDD screening data are supplied courtesy of Eli Lilly and Company—used with Lilly's permission, and gratefully acknowledged. The authors thank T. S. Maskrey (University of Pittsburgh) for project management and technical assistance, S. J. Geib (University of Pittsburgh) for the X-ray analysis of **2**, and J. C. Burnett and R. Cao (University of Pittsburgh) for preliminary K_v7 channel modeling studies.

■ ABBREVIATIONS

KCNQ, potassium channel, voltage-gated, KQT-like subfamily; ADHD, attention deficit hyperactivity disorder; HEK293, human embryonic kidney 293; SAR, structure−activity relationship.

■ REFERENCES

(1) Grunnet, M.; Stroebaek, D.; Hougaard, C.; Christophersen, P. Kv7 Channels as Targets for Anti-Epileptic and Psychiatric Drug-Development. *Eur. J. Pharmacol.* **2014**, *726*, 133−137.

(2) Barrese, V.; Stott, J. B.; Greenwood, I. A. KCNQ-Encoded Potassium Channels as Therapeutic Targets. *Annu. Rev. Pharmacol. Toxicol.* **2018**, *58*, 625−648.

(3) Miceli, F.; Soldovieri, M. V.; Ambrosino, P.; Manocchio, L.; Mosca, I.; Taglialatela, M. Pharmacological Targeting of Neuronal Kv7.2/3 Channels: A Focus on Chemotypes and Receptor Sites. *Curr. Med. Chem.* **2018**, *25* (23), 2637−2660.

(4) Jentsch, T. J. Neuronal KCNQ Potassium Channels: Physiology and Role in Disease. *Nat. Rev. Neurosci.* **2000**, *1*, 21−30.

(5) Li, S.; Choi, V.; Tzounopoulos, T. Pathogenic Plasticity of Kv7.2/3 Channel Activity Is Essential for the Induction of Tinnitus. *Proc. Natl. Acad. Sci. U. S. A.* **2013**, *110*, 9980−9985.

(6) Manville, R. W.; Abbott, G. W. Gabapentin Is a Potent Activator of KCNQ3 and KCNQ5 Potassium Channels. *Mol. Pharmacol.* **2018**, *94*, 1155−1163.

(7) Davoren, J. E.; Claffey, M. M.; Snow, S. L.; Reese, M. R.; Arora, G.; Butler, C. R.; Boscoe, B. P.; Chenard, L.; DeNinno, S. L.; Drozda, S. E.; Duplantier, A. J.; Moine, L.; Rogers, B. N.; Rong, S.; Schuyten, K.; Wright, A. S.; Zhang, L.; Serpa, K. A.; Weber, M. L.; Stolyar, P.; Whisman, T. L.; Baker, K.; Tse, K.; Clark, A. J.; Rong, H.; Mather, R. J.; Lowe, J. A., III Discovery of a Novel Kv7 Channel Opener as a Treatment for Epilepsy. *Bioorg. Med. Chem. Lett.* **2015**, *25*, 4941−4944.

(8) Seefeld, M. A.; Lin, H.; Holenz, J.; Downie, D.; Donovan, B.; Fu, T.; Pasikanti, K.; Zhen, W.; Cato, M.; Chaudhary, K. W.; Brady, P.; Bakshi, T.; Morrow, D.; Rajagopal, S.; Samanta, S. K.; Madhyastha, N.; Kuppusamy, B. M.; Dougherty, R. W.; Bhamidipati, R.; Mohd, Z.; Higgins, G. A.; Chapman, M.; Rouget, C.; Lluel, P.; Matsuoka, Y. Novel Kv7 Ion Channel Openers for the Treatment of Epilepsy and Implications for Detrusor Tissue Contraction. *Bioorg. Med. Chem. Lett.* **2018**, *28*, 3793−3797.

(9) Wu, C.; Gopal, K. V.; Lukas, T. J.; Gross, G. W.; Moore, E. J. Pharmacodynamics of Potassium Channel Openers in Cultured Neuronal Networks. *Eur. J. Pharmacol.* **2014**, *732*, 68−75.

(10) Kalappa, B. I.; Soh, H.; Duignan, K. M.; Furuya, T.; Edwards, S.; Tzingounis, A. V.; Tzounopoulos, T. Potent KCNQ2/3-Specific Channel Activator Suppresses in Vivo Epileptic Activity and Prevents the Development of Tinnitus. *J. Neurosci.* **2015**, *35*, 8829−8842.

(11) Li, S.; Kalappa, B. I.; Tzounopoulos, T. Noise-Induced Plasticity of KCNQ2/3 and HCN Channels Underlies Vulnerability and Resilience to Tinnitus. *eLife* **2015**, *4*, e07242.

(12) Eskioglou, E.; Perrenoud, M. P.; Ryvlin, P.; Novy, J. Novel Treatment and New Drugs in Epilepsy Treatment. *Curr. Pharm. Des.* **2017**, *23*, 6389−6398.

(13) Xu, D.; Penning, T. M.; Blair, I. A.; Harvey, R. G. Synthesis of Phenol and Quinone Metabolites of Benzo[a]Pyrene, a Carcinogenic Component of Tobacco Smoke Implicated in Lung Cancer. *J. Org. Chem.* **2009**, *74*, 597−604.

DOI: 10.1021/acsmedchemlett.9b00097
ACS Med. Chem. Lett. 2019, 10, 929−935

(14) Dousa, M.; Srbek, J.; Radl, S.; Cerny, J.; Klecan, O.; Havlicek, J.; Tkadlecova, M.; Pekarek, T.; Gibala, P.; Novakova, L. Identification, Characterization, Synthesis and HPLC Quantification of New Process-Related Impurities and Degradation Products in Retigabine. *J. Pharm. Biomed. Anal.* **2014**, *94*, 71−76.
(15) Kumar, M.; Reed, N.; Liu, R.; Aizenman, E.; Wipf, P.; Tzounopoulos, T. Synthesis and Evaluation of Potent KCNQ2/3-Specific Channel Activators. *Mol. Pharmacol.* **2016**, *89*, 667−677.
(16) Wipf, P.; Mo, T.; Geib, S. J.; Caridha, D.; Dow, G. S.; Gerena, L.; Roncal, N.; Milner, E. E. Synthesis and Biological Evaluation of the First Pentafluorosulfanyl Analogs of Mefloquine. *Org. Biomol. Chem.* **2009**, *7*, 4163−4165.
(17) Alverez, C.; Arkin, M. R.; Bulfer, S. L.; Colombo, R.; Kovaliov, M.; Laporte, M. G.; Lim, C.; Liang, M.; Moore, W. J.; Neitz, R. J.; Yan, Y.; Yue, Z.; Huryn, D. M.; Wipf, P. Structure-Activity Study of Bioisosteric Trifluoromethyl and Pentafluorosulfanyl Indole Inhibitors of the AAA ATPase p97. *ACS Med. Chem. Lett.* **2015**, *6*, 1225−1230.
(18) Eisenberger, P.; Gischig, S.; Togni, A. Novel 10-I-3 Hypervalent Iodine-Based Compounds for Electrophilic Trifluoromethylation. *Chem. - Eur. J.* **2006**, *12*, 2579−2586.
(19) Southall, N. T.; Ajay. Kinase Patent Space Visualization Using Chemical Replacements. *J. Med. Chem.* **2006**, *49*, 2103−2109.
(20) For information on the, as of 2/1/2019 discontinued, OIDD program, please see https://openinnovation.lilly.com/dd/login.jsp.
(21) Physicochemical properties of agonists were calculated with Instant JChem 18.13.0 (ChemAxon, Cambridge, MA). A HF-6-31G* dihedral angle/conformational energy analysis was performed with Spartan 18 v. 1.3.0 (Wavefunction, Inc., Irvine, CA).
(22) For a related, but antagonist assay set up, see: Priest, B. T.; Cerne, R.; Krambis, M. J.; Schmalhofer, W. A.; Wakulchik, M.; Wilenkin, B.; Burris, K. D. Automated Electrophysiology Assays. In *Assay Guidance Manual*; Sittampalam, S., Coussens, N. P., Brimacombe, K., Grossman, A., Arkin, M., Auld, D., Austin, C., Baell, J., Bejcek, B., Caaveiro, J. M. M., Chung, T. D. Y., Dahlin, J. L., Devanaryan, V., Foley, T. L., Glicksman, M., Hall, M. D., Haas, J. V., Inglese, J., Iversen, P. W., Kahl, S. D., Kales, S. C., Lal-Nag, M., Li, Z., McGee, J., McManus, O., Riss, T., Trask, O. J., Weidner, J. R., Wildey, M. J., Xia, M., Xu, X., Eds. Eli Lilly & Company and the National Center for Advancing Translational Sciences: Bethesda, MD, 2018; pp 493−543; https://www.ncbi.nlm.nih.gov/books/NBK53196/pdf/Bookshelf_NBK53196.pdf.
(23) Schenzer, A.; Friedrich, T.; Pusch, M.; Saftig, P.; Jentsch, T. J.; Groetzinger, J.; Schwake, M. Molecular Determinants of KCNQ (Kv7) K+ Channel Sensitivity to the Anticonvulsant Retigabine. *J. Neurosci.* **2005**, *25*, 5051−5060.
(24) Kim, R. Y.; Yau, M. C.; Kurata, H. T.; Galpin, J. D.; Ahern, C. A.; Seebohm, G.; Pless, S. A. Atomic Basis for Therapeutic Activation of Neuronal Potassium Channels. *Nat. Commun.* **2015**, *6*, 8116.
(25) *Spartan'10*; Wavefunction, Inc.: Irvine CA. Calculations performed using the PM6 semiempirical parametrization set.
(26) Wang, A. W.; Yang, R.; Kurata, H. T. Sequence Determinants of Subtype-Specific Actions of KCNQ Channel Openers. *J. Physiol.* **2017**, *595*, 663−676.
(27) Meanwell, N. A. Fluorine and Fluorinated Motifs in the Design and Application of Bioisosteres for Drug Design. *J. Med. Chem.* **2018**, *61*, 5822−5880.
(28) Greenwood, I. A.; Ohya, S. New Tricks for Old Dogs: KCNQ Expression and Role in Smooth Muscle. *Br. J. Pharmacol.* **2009**, *156*, 1196−1203.
(29) Wang, L.; Qiao, G.-H.; Hu, H.-N.; Gao, Z.-B.; Nan, F.-J. Discovery of Novel Retigabine Derivatives as Potent KCNQ4 and KCNQ5 Channel Agonists with Improved Specificity. *ACS Med. Chem. Lett.* **2019**, *10*, 27−33.

DOI: 10.1021/acsmedchemlett.9b00097
ACS Med. Chem. Lett. 2019, 10, 929−935